

Transverse momentum fluctuation in ultra-central Pb+Pb collision at the LHC

Rupam Samanta^{1,2,*}, Somadutta Bhatta³, Jianguyong Jia^{3,4}, Matthew Luzum⁵, and Jean-Yves Ollitrault².

¹AGH University of Science and Technology, Faculty of Physics and Applied Computer Science, aleja Mickiewicza 30, 30-059 Cracow, Poland

²Université Paris Saclay, CNRS, CEA, Institut de physique théorique, 91191 Gif-sur-Yvette, France

³Department of Chemistry, Stony Brook University, Stony Brook, NY 11794, USA

⁴Physics Department, Brookhaven National Laboratory, Upton, NY 11976, USA

⁵Instituto de Física, Universidade de São Paulo, Rua do Matão, 1371, Butantã, 05508-090, São Paulo, Brazil

Abstract. The ATLAS collaboration has recently observed that the variance of the transverse momentum per particle ($[p_t]$), when measured as a function of the collision multiplicity (N_{ch}) in Pb+Pb collisions, decreases by a factor 2 for the largest values of N_{ch} , corresponding to ultra-central collisions. We show that this phenomenon is naturally explained by invoking impact parameter (b) fluctuations, which contribute to the variance, and gradually disappear in ultra-central collisions. It implies that N_{ch} and $[p_t]$ are strongly correlated at fixed b , which is explained by the local thermalization of the QGP medium.

1 Introduction

The left panel of Fig. 1 displays the variance of transverse momentum per particle ($[p_t]$) as a function of the collision multiplicity in Pb+Pb collisions at the LHC [1]. (It is the dynamical contribution to the variance, after subtracting the trivial statistical fluctuation from the finite multiplicity.) It decreases over a narrow range of multiplicity around $N_{ch} = 3700$. This phenomenon is not explained by models such as HIJING, which predicts a smooth $1/N_{ch}$ dependence of the variance for all ranges of N_{ch} [2]. We show that it is naturally explained if the medium produced during the collision thermalizes.

2 Hydro vs HIJING results

The impact parameter of the collision, b , is not measured, and varies event by event. Fluctuations observed in a sample of collisions event originate from fluctuations of b , and from fluctuations at fixed b . In order to understand their respective roles, we run simulations of Pb+Pb collisions at 5.02 TeV at fixed b , more specifically at $b = 0$.

First, we simulate 150 events using relativistic viscous hydrodynamics [3] and compute N_{ch} and $[p_t]$ in each event. Fig. 1 displays the distribution of the two quantities from hydrodynamic simulation where thermalization of the QGP is assumed. It is clearly visible that

*e-mail: rsamanta@agh.edu.pl

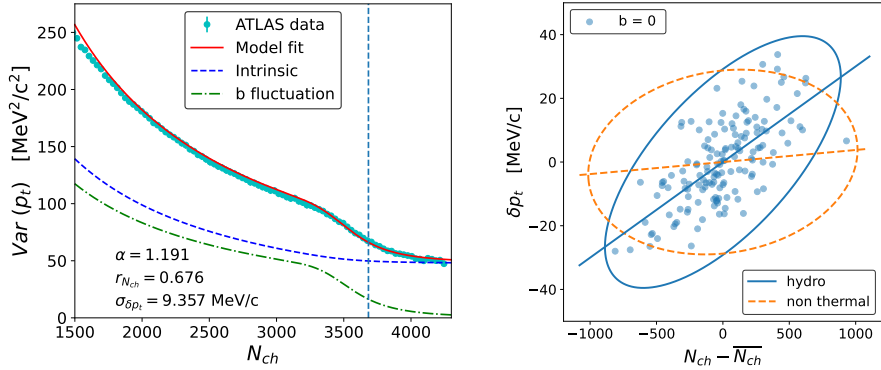


Figure 1. Left: ATLAS data (light blue symbols) and our model fit presented in Sec.3 (solid red curve). The green curve denotes the contribution due to b fluctuation and the blue dashed line denotes the contribution of intrinsic fluctuation. The vertical dashed line is the knee of the multiplicity distribution. Right : Two dimensional distribution of $[p_t]$ and N_{ch} from simulation of Pb+Pb collisions at 5.02 TeV and $b=0$. Blue symbols are hydrodynamic calculations. Instead of $[p_t]$ and N_{ch} , we plot the differences $N_{ch} - \overline{N_{ch}}$ and $\delta p_t = [p_t] - \overline{p_t}$ where $\overline{N_{ch}} = 6692$ and $\overline{p_t} = 1074 \text{ MeV}/c$ are the average values. The blue curve is the 99% confidence ellipse of a Gaussian distribution fitted to these symbols. The orange curve is a similar 99% confidence ellipse for 1.4×10^6 collisions simulated with HIJING. The straight lines represent the average values $\delta p_t(N_{ch}, b = 0)$.

both $[p_t]$ and N_{ch} have significant fluctuation. As the impact parameter is fixed, the origin of these fluctuations is purely quantum, due to genuine intrinsic fluctuation at the initial state of the collision.

Most importantly, there is a strong positive correlation between $[p_t]$ and N_{ch} , whose physical origin is clear: Larger N_{ch} means larger density N_{ch}/V , as the collision volume, which is mostly defined by the impact parameter of the collision, is fixed. A larger density results in a larger initial temperature if the system thermalizes. This in turn implies a higher energy per particle in the final state, and eventually a larger transverse momentum per particle $[p_t]$, generating the positive correlation between $[p_t]$ and N_{ch} .

Second, we run simulations using the HIJING model [4], which considers the collision as a superposition of independent nucleon-nucleon collision, and in which the particles have no interaction between each other after production. The striking difference in comparison to the hydro results is that the correlation between N_{ch} and $[p_t]$ is smaller by a factor ~ 10 . In HIJING, a larger density does not imply a significant increase of $[p_t]$, which can be ascribed to the lack of thermalization.

3 Model fit

We model fluctuations of $[p_t]$ by assuming that the joint probability distribution of $[p_t]$ and N_{ch} at fixed b is a two-dimensional correlated Gaussian [5], denoted by $P([p_t], N_{ch}|b)$. It is characterized by five parameters: mean and variance of $[p_t]$ and N_{ch} , denoted by $\overline{p_t}(b)$, $\overline{N_{ch}}(b)$, $\text{Var}(p_t|b)$, $\text{Var}(N_{ch}|b)$ and the Pearson correlation coefficient between $[p_t]$ and N_{ch} , $r_{N_{ch}}(b)$ which we expect to be positive in hydrodynamics, as shown in Fig. 1 (right).

The mean and variance of N_{ch} are obtained by fitting the measured distribution of N_{ch} as a superposition of Gaussians, along the lines of Ref. [6]. The average value of N_{ch} at $b = 0$ is the knee of the distribution, which is reconstructed precisely. Note that the fall of the variance in Fig. 1 precisely occurs around the knee.

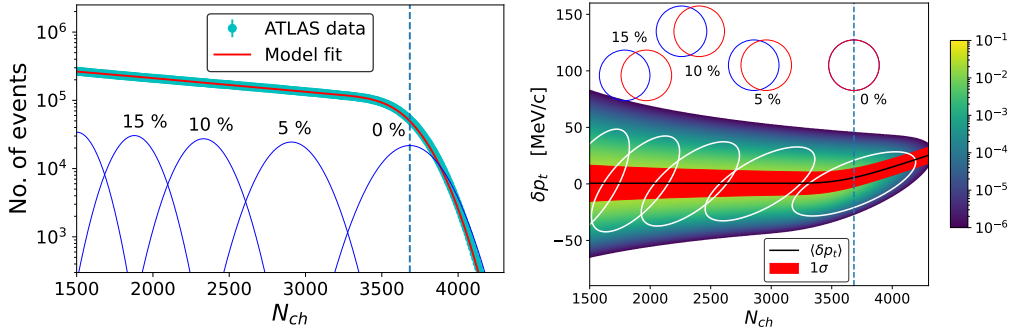


Figure 2. Left : Charged particle multiplicity (N_{ch}) distribution in Pb+Pb collision at 5.02 TeV measured by the ATLAS collaboration, denoted by the light blue symbols. The solid red line represents the model fit. The thin blue lines corresponds to the Gaussian distributions $P(N_{ch}|b)$ drawn for 0 %, 5 %, 10 % and 15 % centrality fractions. The vertical dashed line corresponds to the "knee" ($\overline{N_{ch}b} = 0$) of the distribution. Right: Two dimensional joint distribution of transverse momentum per particle [p_t] and multiplicity N_{ch} returned by the model fit to the fluctuation data. Rather than plotting [p_t], we plot $\delta p_t = [p_t] - \overline{p_t}(0)$. The white curves represent the 99 % confidence ellipses at fixed impact parameters. Corresponding to these values b , a schematic representation of the colliding nuclei is shown. The solid black line denotes the mean value of δp_t averaged over events and the red band represents $1\text{-}\sigma$ band.

The mean transverse momentum $\overline{p_t}(b)$ is essentially independent of b for 30 % most central collisions [7]. We subtract this constant and only study the distribution of the distribution of $\delta p_t = [p_t] - \overline{p_t}$. We assume that the variance $\text{Var}(p_t|b)$ varies with the mean according to a power law, $\text{Var}(p_t|b) = \sigma_{\delta p_t}^2 (\overline{N_{ch}}(0)/\overline{N_{ch}}(b))^\alpha$, where α and $\sigma_{\delta p_t}$ are constants [5]. For simplicity, we assume the correlation $r_{N_{ch}}$ to be independent of b .

The variance of δp_t at fixed N_{ch} is then evaluated in the following way. We first obtain the distribution of δp_t at fixed N_{ch} and b using $P(\delta p_t|N_{ch}, b) = P(\delta p_t, N_{ch}|b)/P(N_{ch}|b)$. It is again a Gaussian distribution, therefore, it is fully characterized by its mean and variance, which we denote by κ_1 and κ_2 . Both are functions of N_{ch} and b . The crucial point is that the mean κ_1 is proportional to the multiplicity fluctuation $N_{ch} - \overline{N_{ch}}(b)$. It is proportional to the Pearson correlation coefficient $r_{N_{ch}}$ between δp_t and N_{ch} (straight blue line in Fig. 1 right).

The last step is to average over b . For this, one needs the probability distribution of b at fixed N_{ch} , which is obtained using Bayes' theorem $P(b|N_{ch})p(N_{ch}) = P(N_{ch}|b)P(b)$ along the lines of Ref. [6]. A simple calculation then shows that

$$\begin{aligned} \text{mean } \langle \delta p_t \rangle &= \langle \kappa_1 \rangle_b \\ \text{Var}(p_t) &= (\langle \kappa_1^2 \rangle_b - \langle \kappa_1 \rangle_b^2) + \langle \kappa_2 \rangle_b \end{aligned} \quad (1)$$

where angular brackets $\langle \dots \rangle_b$ denote the average over b for fixed N_{ch} . Two terms contribute to the variance: The first term originates from fluctuations of the impact parameter b at fixed N_{ch} , and the second term is the true intrinsic (quantum) fluctuation, which is not the by-product of b fluctuation.

The expression in Eq. (1) is finally fitted to ATLAS data using the three parameters : $\sigma_{\delta p_t}$, $r_{N_{ch}}$ and α . Fig. 1 displays the model fit to the data (red lines) and the two separate contributions to $\text{Var}(p_t|N_{ch})$. Our model precisely explains the steep decrease of the variance around the knee. Below the knee, both contributions have comparable magnitudes, but above the knee, the first term, due to impact parameter fluctuations, gradually disappears, causing the steep fall in the variance data. This occurs because the effect of b fluctuation becomes

negligible in ultra-central region due to the strict lower limit of b (≥ 0), where the distribution of δp_t becomes a truncated Gaussian [6, 8].

Fig. 2 displays the two-dimensional distribution of $[p_t]$ and N_{ch} returned by our fit. The white curves represent 99% confidence ellipses at fixed impact parameters and they are tilted with respect to the horizontal axis as in the hydrodynamic calculation in Fig. 1. The tilts denote the positive correlation between $[p_t]$ and N_{ch} , characterized by $r_{N_{ch}}$. From this plot, it can be seen that the width of $[p_t]$ distribution is partly because several ellipses contribute at a given N_{ch} (first term in Eq. 1) and the other part comes from the vertical width of a single ellipse (second term in Eq. 1). As a corollary, we also predict a slight increase of the mean transverse momentum $\langle \delta p_t \rangle$ with N_{ch} , denoted by the black line in Fig. 2.

4 Physical significance and thermodynamic interpretation

Our results imply that there is a strong correlation between $[p_t]$ and N_{ch} at fixed impact parameter, which is quantified by the Pearson correlation coefficient $r_{N_{ch}} = 0.676$. As explained in Sec. 2, such a correlation is naturally present in a hydrodynamic description. Hence, the recent ATLAS data further support the common hypothesis that local thermalization is achieved in Pb+Pb collisions. It is the first such evidence which does not involve anisotropic flow.

Additionally, our analysis and methodology pave the way to separate the classical (geometrical) and quantum (intrinsic) fluctuation. Moreover, the slight increase of mean transverse momentum with multiplicity could be used to extract the speed of sound in QGP medium [9], which has recently been measured by the CMS collaboration with great precision [10].

Acknowledgments

R. S. is supported by the Polish National Science Center under grant NAWA PRELUDIUM BIS: PPN/STA/2021/1/00040/U/00001 and PRELUDIUM BIS: 2019/35/O/ST2/00357. S.B and J.J are supported by DOE DE-SC0024602. M. L. thanks the São Paulo Research Foundation (FAPESP) for support under grants 2021/08465-9, 2018/24720-6, and 2017/05685-2, as well as the support of the Brazilian National Council for Scientific and Technological Development (CNPq).

References

- [1] G. Aad et al. (ATLAS), Phys. Rev. C **107**, 054910 (2023), 2205.00039
- [2] S. Bhatta, C. Zhang, J. Jia, Phys. Rev. C **105**, 024904 (2022), 2112.03397
- [3] P. Bozek, R. Samanta, Phys. Rev. C **105**, 034904 (2022), 2109.07781
- [4] M. Gyulassy, X.N. Wang, Comput. Phys. Commun. **83**, 307 (1994), nucl-th/9502021
- [5] R. Samanta, S. Bhatta, J. Jia, M. Luzum, J.Y. Ollitrault (2023), 2303.15323
- [6] S.J. Das, G. Giacalone, P.A. Monard, J.Y. Ollitrault, Phys. Rev. C **97**, 014905 (2018), 1708.00081
- [7] S. Acharya et al. (ALICE), Phys. Lett. B **788**, 166 (2019), 1805.04399
- [8] R. Samanta, J.a.P. Picchetti, M. Luzum, J.Y. Ollitrault, Phys. Rev. C **108**, 024908 (2023), 2306.09294
- [9] F.G. Gardim, G. Giacalone, J.Y. Ollitrault, Phys. Lett. B **809**, 135749 (2020), 1909.11609
- [10] Tech. rep., CMS preliminary, presented in Quark Matter (2023), <https://cds.cern.ch/record/2870141>